Available online at www.scholarsresearchlibrary.com

Scholars Research Library

Der Pharmacia Lettre, 2016, 8 (6):170-181
(http://scholarsresearchlibrary.com/archive.html)

ISSN 0975-5071
USA CODEN: DPLEB4

Synthesis of zinc oxide nanorods on platinum wire & fabrication of triglyceride biosensor

Rekha Dhull, Kavita Rathee and Sandeep Singh*

Department of Bio of Biochemistry, Maharshi Dayanand University, Rohtak 124001, India

---

ABSTRACT

In the present study platinum (Pt) wire has been used as a substrate for the synthesis of zinc oxide nanorods. Aqueous Chemical Growth method has been used for the successful synthesis of ZnO nanorods on the platinum wire. The synthesis has been confirmed by various analytical techniques. The characterization has also been done by UV-Vis Spectroscopy, X-Ray Diffraction (XRD), Field Effect Scanning Electron Microscopy (FESEM), Fourier Transform Infrared Spectroscopy (FTIR) and Electrochemical Impedance Study (EIS). The above said characterization techniques confirmed the optical, structural constituency, bending vibrations of bond formation and electrical conductivity of the synthesized nanorods. The newly developed biosensor showed linearity ranging from 10 µM to 250 µM with a minimum detection limit of 10 µM. This method also showed a good correlation coefficient (r) 0.983.

Keywords: Platinum wire, Zinc Oxide (ZnO), Nanorods, XRD, FTIR, FESEM.

INTRODUCTION

Zinc Oxide (ZnO), EC number 215-222-5 is available in surroundings as zincite mineral. It is present in crystalline white powder form which is water insoluble. The Crystalline powder possesses piezoelectric nature which on heating turns its colour from white to yellow [1–3]. The above said nanostructures can be easily synthesized in different forms which include nanoparticles, nanorods, nanowires, nanobelts etc. according to the need. Different methods are available for successful synthesis of nanorods on a variety of substrates. Vapour- Liquid- Solid method of synthesizing nanomaterials has also been used for various materials and variety of supports [4,5]. Some of the other methods are micro-emulsion, aerosol, conventional ceramic-fabrication, ultrasonic, evaporation of solutions and suspensions, wet chamber, evaporative decomposition of solution, sol-gel method, solid state reaction, synthesis and spray pyrolysis [6,7]. ZnO nanomaterials have variety of applications in different fields due to their high electrical conductivity having band gap of 3.37 eV and high excitation binding energy of 60 meV at room temperature [8]. It is also used as corrosion inhibitor pigments used as organic coatings for preventing the surface from corrosion [9]. ZnO is also used as catalysts in reactions, electronics devices, optoelectronics and photochemistry due to their invaluable characteristics as semiconductors [10, 11].

A lot of work has been done on ZnO nanostructures for exploiting its application in sensing field, a variety of properties of ZnO are exploited for fabrication of different nano sensors; they are also used for development of gas sensors which are based on the capability in sensing changes which take place with respect to conductance as it is a reversible chemisorption process of gases reacting on ZnO nano surface [12]. The piezoelectric properties of ZnO are advantageous in sensing the changes occurring with respect to pressure [13]. It is also biocompatible and nontoxic compound so it can be used for fabricating the biosensors [14] and their application in various diagnostic fields.

Among all the nanostructures ZnO nanorods are less exploited. So in the present investigation we have synthesized the ZnO nanorods on the platinum substrate and successfully used for the fabrication of triglyceride biosenor. The aqueous chemical growth [15] method was used with modifications for the easy and less time consuming growth of ZnO nanorods on the Au wire. The overview of the synthesis process is shown below as Scheme 1.

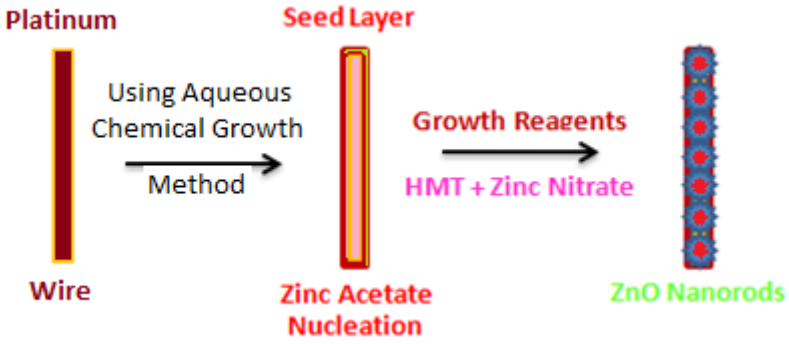

Scheme 1: ZnO nanorod synthesis process

MATERIALS AND METHODS

2.1 Reagents

The working electrode Platinum Wire (Pt wire) of approx. 1 mm diameter and 2 inch length was obtained from local market. The reagents such as Zinc Acetate, Hexamethylene Tetramine (HMT, $C_6H_{12}N_4$), Zinc Nitrate (Zn $(NO_3)_2.6H_2O$), Alumina and Piranha Solution, trioline were used without any further pre-treatment and all were purchased from SRL, Mumbai. All solutions were prepared by using Distilled Water (DW) in this study.

2.2 Apparatus

Spectrometric measurements for characterization of synthesized Zinc Oxide (ZnO) Nanorods were performed using Shimadzu cooperation UV 2450 spectrophotometer at Centre for Biotechnology, Maharshi Dayanand University, Rohtak. Fourier transform infrared spectroscopy (FTIR) was performed at Advanced Instrumentation Research Facility (AIRF), JNU, New Delhi. Field Emission Scanning Electron Microscopy (FESEM) was carried out at University of Minho, Braga, Portugal. Structural characteristics of prepared ZnO nanorods was studied by X-ray diffractometer (XRD) showing diffraction peaks were carried out at Department of Physics, Maharshi Dayanand University, Rohtak. Autolab electrochemical analyser Model PGSTAT 12/30/302 was used for Electrochemical Impedance Study (EIS).

2.3 Synthesis of ZnO Nanorods

Platinum wire surface was firstly pre cleaned with ethanol and distilled water and was then polished with 0.05mM of alumina slurry. After this preliminary cleaning step about 0.05mM of alumina slurry was used for polishing the pre cleaned surface of Pt wire. Pt wire was then dipped for about 10 min in piranha solution which consisted of hot mixed solution of 30% Hydrogen Peroxide (H_2O_2) and concentrated Sulphuric Acid (H_2SO_4), in a ratio of 3:1 (v/v). Distilled water was then used for ultrasonic cleaning of the Pt surface. Spin Coating Method was then used to deposit layer of Zinc Acetate on Pt wire. In this process centrifugation was done for 20 to 30 minutes at 6000 rpm in Zinc Acetate solution to obtain a homogenous layer on the Pt surface. In order to obtain homogeneous deposition of Zinc Acetate throughout the Pt surface the spin-coating was repeated for about 5 times. This process of homogeneous deposition of zinc acetate layer served as nucleation sites for the proper growth and alignment of ZnO nanorods on the surface of Pt wire.

The Pt wire was heated in an oven for about 15 minutes at 130°C. ZnO nanorods were grown using aqueous chemical growth method which involved mixing of equimolar concentration (0.025-0.01 M) of zinc nitrate (Zn $(NO_3)_2.6H_2O$) and hexamethylene tetramine (HMT, $C_6H_{12}N_4$) in double distilled water. Pt wire was then dipped in this solution and heated for 4 to 5 hrs at a temperature of 90°C. The reaction scheme involved in aqueous chemical growth method of ZnO nanorods is shown below.

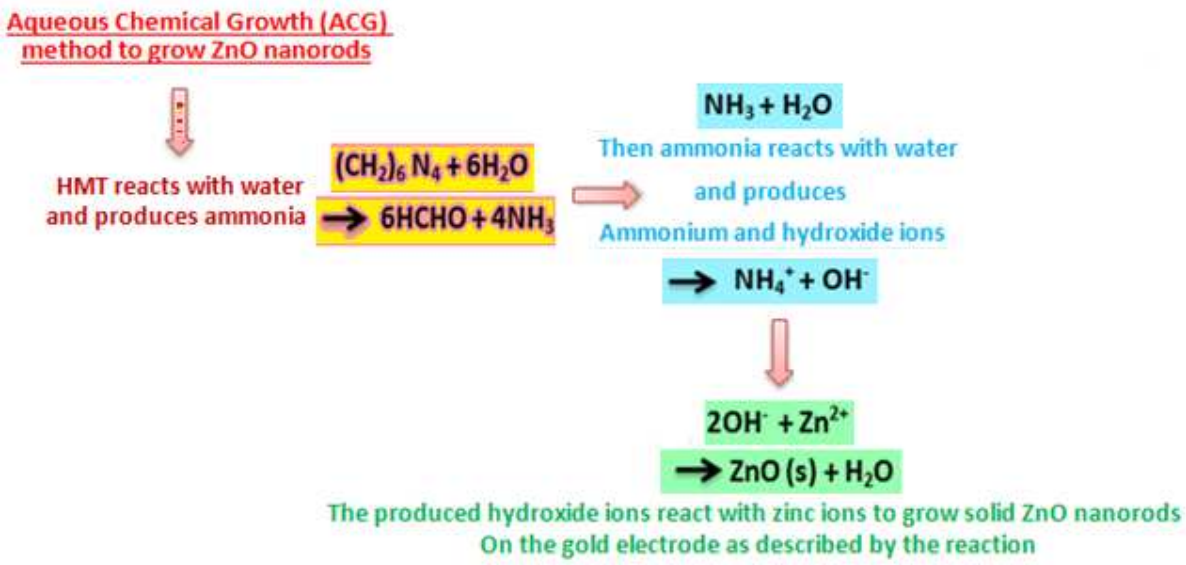

Scheme 2: Reaction scheme of aqueous chemical synthesis of ZnO nanorods

2.4 Physical Characterization of chemically synthesized ZnO Nanorods

The study of grown ZnO nanorods was then carried out by using different techniques such as UV visible spectroscopy, XRD, FTIR and FESEM. Characterization of nanorods was done on the basis of their morphological structure, chemical bonding involved, size and crystal structure. Field emission scanning electron microscopy (FESEM) was carried out for morphological study of grown ZnO nanostructures on Pt wire. XRD was performed to investigate the crystalline structure. FTIR study was carried out by using Varian 7000 to determine elemental and chemical constituents of the synthesized nanorods. Shimadzu cooperation UV 2450 was used as UV visible spectrometer to study the absorbance of the grown ZnO nanorods.

2.5 Assembly of Triglyceride Biosensor

After the completion of fabrication process, the fabricated devices will be cleaned with deionized-water. For aminosilanization of the ZnO surface, it is necessary to attach OH group on the ZnO surface. So, APS, Distilled Water and 95% Ethanol in the ratio of 2:3:95 will be prepared. Then the ZnO nanorods will be smeared with 1ml of the above solution and dried at room temperature for 1hour followed by washing with DW and dried in air. Next, ZnO nanorods will be immersed in 0.01 M PBS with 20 mM glutaraldehyde, which will act as a linker material between the enzyme and the APS-treated ZnO surface, at 4°C for 2 h. For enzyme immobilization, mixture of lipase and glycerol dehydrogenase at a concentration of 1 mg/ml in 0.01 M PBS will be dropped onto the surface of ZnO nanowires of one electrode. The enzyme bound working electrode along with the two electrodes i.e. Ag/AgCl electrode (reference electrode) and Pt counter current electrode will constitute the basic working assembly of electrochemical cell. These electrodes will be connected through potentiostat/galvanostat.

For dehydrogenase based system, reaction solution will consist of 1ml of 2.26mM triolein in 14ml 0.1M sodium phosphate buffer, pH 7.0, containing 10mM NAD^+. When the analyte triglyceride is present in the sample, the triglycerides will be converted into glycerol and fatty acids. Then glycerol will be oxidized by the action of the glycerol dehydrogenase (GlyDH) into Dihydroxyacetone and NAD will be reduced to NADH. On the electrode surface, NADH will be oxidized and the oxidation current will be directly proportional to the triglyceride concentration in the solution

$$\text{Triglyceride} + 3H_2O \xrightarrow{\text{Lipase}} \text{Glycerol} + 3\ \text{Fatty Acids}$$

$$\text{Glycerol} + NAD^+ \xrightarrow{\text{GlyDH}} \text{Dihydroxyacetone} + NADH + H^+$$

$$NADH \xrightarrow{E} NAD^+ + H^+ + 2e^-$$

2.6 Study of electrochemical behaviour of working electrode

Electrochemical measurements were made using there electrode system with Lipase/Glycerol dehydrogenase - glutaraldehyde-APS-nanoZnO-Pt electrode as working electrode, reference electrode (Ag/AgCl) and counter current

electrode (Pt wire). Equilibration of working electrode was done at 0.6 V before each run until steady-state current was obtained at + 0.6V. Electrochemical reaction involved during measurement is shown as under:

2.7 Kinetic properties of Lipase/Glycerol dehydrogenase -glutaraldehyde-APS-nanoZnO-Pt

The following kinetic properties of fabricated working electrode were studied: optimum pH, incubation temperature, incubation time, effect of substrate (ascorbic acid) concentration and calculation of K_m and V_{max} from Line weaver - Burk plot. To determine optimum working pH of working electrode, the pH of reaction buffer was varied from 3.0-6.5 using the following buffer, each at a final conc. of 0.1M: pH 3.5 to 5.0 sodium citrate and pH 3.0 to 6.5 sodium acetate buffers. Similarly, for optimum temperature, the reaction mixture was incubated at different temperatures ranging from 15 to 45˚C at interval of 5˚C. Time of incubation was also studied from 5 min to 35 min at a regular interval of 5 min. To study the effect of substrate concentration on the working electrode, assays were performed up to 500 µM. K_M and V_{max} values for immobilized enzyme were calculated from Lineweaver-Burk plot between reciprocal of substrate concentration [1/S] and reciprocal of initial velocity of the reaction [1/V].

2.8 Evaluation of the present method

The new method was evaluated as follows:

2.8.1 Linearity and minimum detection limit: The linearity and minimum detection limit was calculated by correlating the values with standard graph.

2.8.2 Analytical recovery: To study analytical recovery, 1 µM and 2 µM of trioline was added to the sample solution. The concentration of ascorbic acid in sample was determined by the present method before and after the addition of trioline. The percent analytical recovery of added ascorbic acid was determined.

2.8.3 Precision: To assess the reproducibility and repeatability of the present method, trioline concentration in the sample was determined 6 times on same day (within batch). In another experiment, trioline was determined on day 1 and day 7 after storing samples at -20˚C (between batch) employing present method. The coefficients of variation (CV) for within and between batch were determined using the formula given-

$$CV = \frac{\sigma \times 100}{a}$$

Where, σ = standard deviation, and a = mean of series

The standard deviation (σ) was calculated as-

$$\sigma = \sqrt{(\Sigma(\chi - \bar{\chi})^2 / n - 1}$$

2.8.4 Accuracy: To evaluate the accuracy of the present method, the trioline concentration in 5 samples was determined by the present method and compared with those obtained by standard method. The regression plot between the two methods were drawn and the correlation coefficient was determined by using following formula-

$$r = \frac{n\Sigma xy - \Sigma x \Sigma y}{\sqrt{n\Sigma x^2 - (\Sigma x)^2}\ \sqrt{n\Sigma y^2 - (\Sigma y)^2}}$$

Where, x = trioline values by standard method, and y = trioline values by present method.

2.8.5 Interference study

The response of the present method was checked in the presence of potential interfering compounds such as starch, glucose, sucrose, fructose and urea each at a concentration of 0.1 mM.

2.9 Reusability and storage stability of enzyme rod

To reuse the enzyme rod, it was washed by washing buffer (0.01 M Phosphate buffer saline, pH-7.2 with 0.1% tween-20). The long-term storage stability of the working electrode was investigated over a two month period. The activity of immobilized enzymes was measured once in every 6 days.

RESULTS AND DISCUSSION

3.1. UV Visible Spectroscopy of Synthesized Nanorods

Shimadzu cooperation UV 2450 spectrophotometer was used for spectroscopy study of the optical properties of the grown nanorods ZnO structure. An absorbance UV peak was observed at 370 nm which corresponded for the presence of ZnO as depicted in fig. 1. This confirmed that the synthesized material was ZnO.

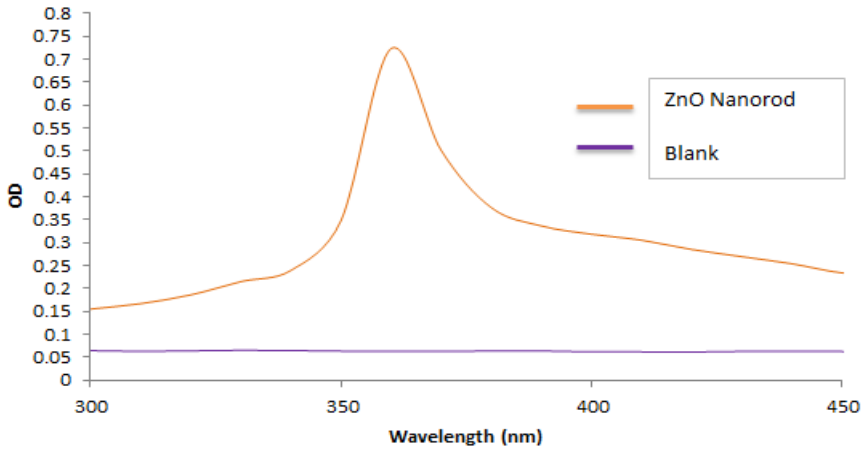

Fig. 1: UV Visible absorption spectra of ZnO Nanorods

3.2. X-Ray Diffraction Analysis of ZnO

X-ray diffraction (XRD) characterization technique was conducted in order to determine the crystalline structure and the crystal plane of the synthesized ZnO nanorods. The diffraction pattern of the ZnO nanorods is shown in Fig. 2. The XRD diffraction pattern peaks were at 31.6°, 34.2°, 36.4º, 47.4º, 56.7º, 63.2º, 66.7º, 68.2º and 69.2° were obtained which were designated to (100), (002), (101), (102), (110), (103), (200), (112) and (201) respectively. These XRD peaks are specific diffraction peaks for ZnO crystalline plane and are in agreement with JCPDS card no. 089-3697. The XRD well defined peaks showed that the synthesized ZnO nanorods were pure with no impurities and were in quartzite hexagonal phase.

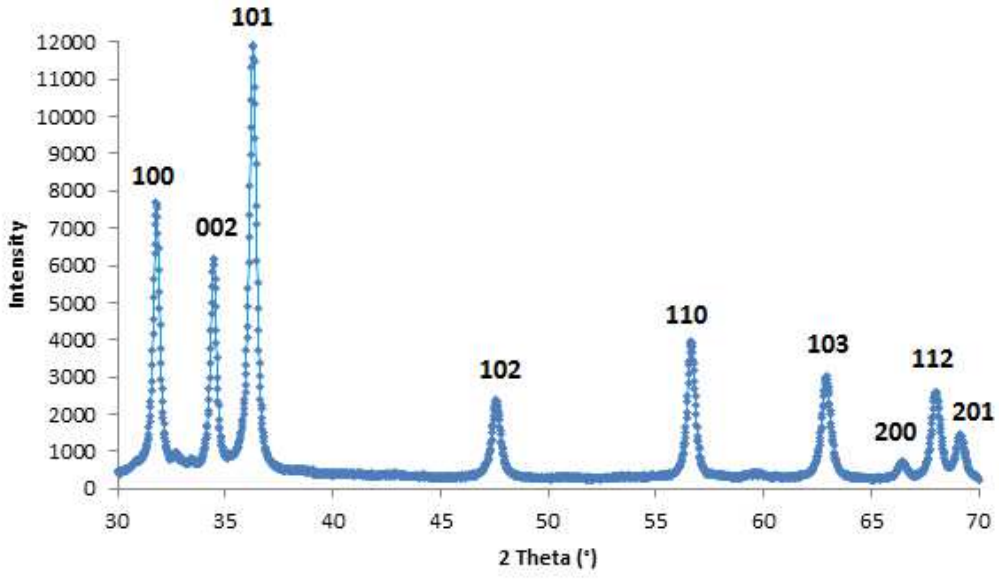

Fig. 2: XRD pattern obtained from ZnO nanorods

3.3. Fourier transform infrared spectroscopy (FTIR) analysis of ZnO nanorods

FTIR analysis was conducted in order to the study the chemical bonding involved in the ZnO nanorods. The FTIR spectrum of the ZnO nanorods is shown in Fig. 3. The peak at 520 cm^{-1} corresponds to the wurtzite hexagonal phase of synthesized pure ZnO. Several other additional peaks were obtained at 520 cm^{-1}, 1381 cm^{-1}, 1541 cm^{-1}, 2912 cm^{-1} and 3381 cm^{-1}. Theses peaks correspond to the chemical bonding present. Peak at 1381 cm^{-1} and 1541 cm^{-1} were due

to presence of carboxylate group (COO^-) bond stretching. This COO^- group is due to use of zinc acetate during the synthesis of ZnO nanorods. The peak at 2912 cm^{-1} was due to O-H bond stretch and peak at 3381 cm^{-1} was due to bending vibrations of C-H stretch.

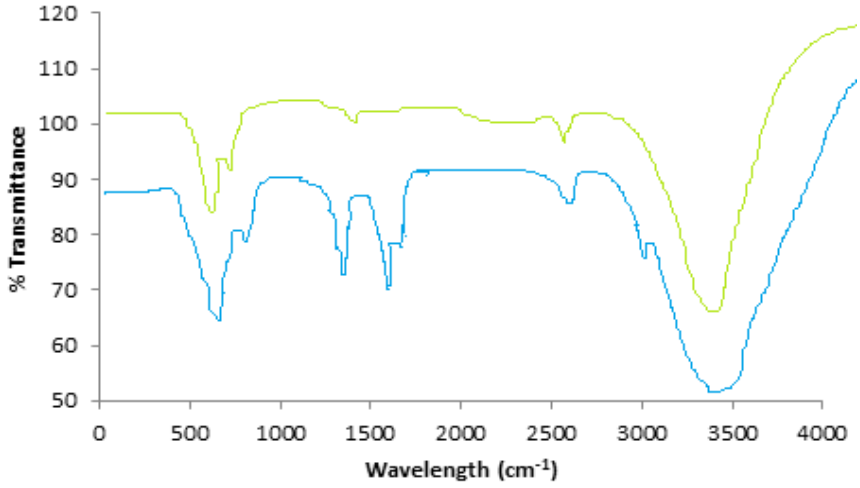

Fig. 3: FTIR of synthesized ZnO showing signature peaks

3.4 Field Emission Scanning Electron Microscopy (FESEM) of synthesized ZnO Nanorods

FESEM was used to study morphological characteristics of ZnO nanorods at different stages of chemical growth of nanorods. In fig 4a image of bare Pt wire without any chemical pre-treatment and showing no growth had been depicted with uniform morphology. Fig. 4b, showing the growth on the Pt wire surface of ZnO nanorods. The presence of rod like structures on Pt surface confirmed successful deposition of ZnO nanorods. The size of synthesized nanorods was determined and was found in nano range scale in fig 4c. The fully grown nanorods exhibited rod-like shape with hexagonal cross section.

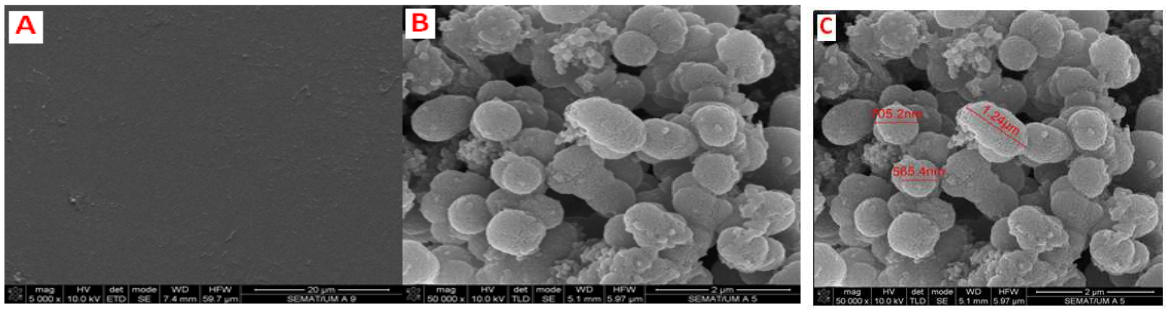

Fig. 4: SEM images of (a) Pt wire without chemical pre-treatment, (b) start of growth of ZnO nanorods on Pt surface and (c) Size of lab synthesized nanorods

3.5 Electrochemical Impedance studies (EIS) of synthesized ZnO Nanorods

The change in charge transfer during the different steps involved in chemical deposition of ZnO nanorods at Pt wire surface was studied using Electrochemical Impedance. Nyquist plot was used to determine the correlation between Resistive charge transfer (R_{CT}) and chemically modified surface of Pt. Mixed kinetic and diffusion control circuit model was used to analyse the process occurring at the interface of nanorods synthesized. For this study phosphate buffer (0.2 M, pH 7.5) with mixture of $[Fe(CN)_6]^{3-}$ & 0.1 mM $[Fe(CN)_6]^{4-}$ (0.1mM). The frequency range was from 0.01 Hz to 10 KHz while recording the impedance. EIS of bare Pt wire surface showed almost straight line which is the limited diffusion step with R_{CT} value of 150 Ω (Fig. 5 curve a). The R_{CT} value decreases to 120 Ω after deposition of seed layer by nucleation of zinc acetate on bare Pt wire, this implies that the electrical conductivity is increased and hindrance is low (Fig. 5 curve b). Further with the chemical synthesis of ZnO on the seed layer of ZnO, the R_{CT} value increased to 180 Ω. This was due to increment of hindrance during charge transfer by growth of ZnO nanorods (Fig. 5 curve c). This proved the successful growth of ZnO nanorods on the Pt surface.

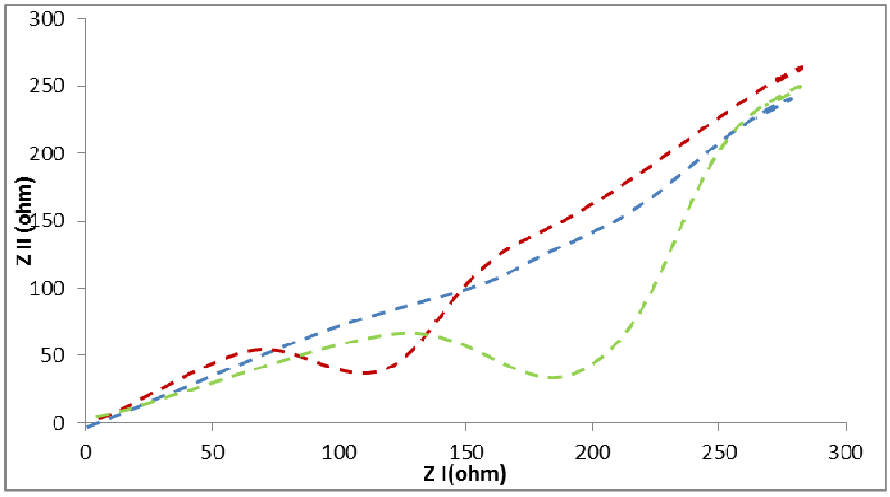

Fig. 5: Electrochemical Impedance of (a) Pt wire (without chemical modification), (b) Pt surface with zinc acetate seed layer (c) Pt wire with fully developed ZnO nanorods. Inset showing mixed kinetic and diffusion control circuit

1.6 Morphological studies of working electrode

Morphological characterization was done by SEM. Figure 6a showing SEM image of APS-nanoZnO-Pt. This showed mesh like morphology which confirmed successful deposition of nanomaterial on bare Pt electrode. Figure 6b showing morphology of final working electrode APS-nanoZnO-Pt with immobilized enzyme.

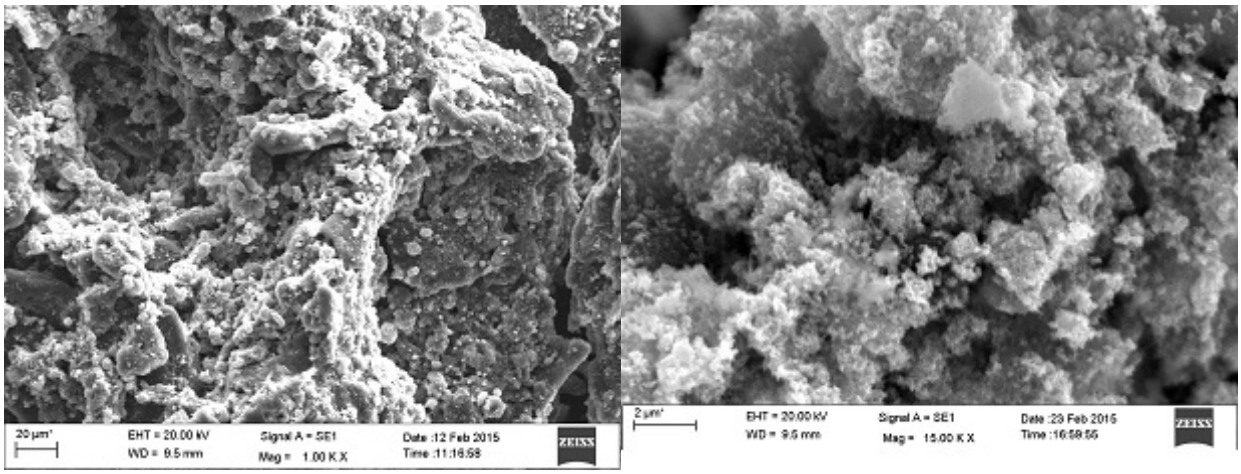

Figure 6. SEM images of (a) APS-nanoZnO-Pt (b) Enzyme-APS-nanoZnO-Pt

3.7 Cyclic Voltammetric Study of Ascorbate Biosensor

CV was performed for electrochemical studies of nanomaterial based working electrode. CV was carried out in presence of trioline (250 µL, 0.05 mM) in phosphate buffer (pH 7.0) with 10 mVs^{-1} scan rate. Figure 7 showed the CV of bare Pt (curve a) wire with no peak. Curve b showed oxidation peak at +0.370 mA of trioline by enzyme immobilized working electrode i.e., Lipase/Glycerol dehydrogenase -glutaraldehyde-APS-nanoZnO-Pt electrode.

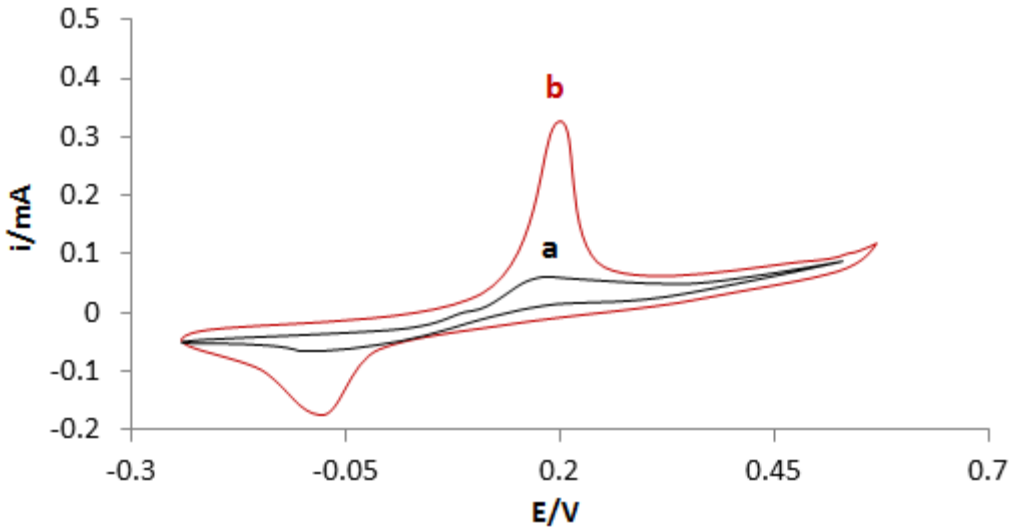

Figure 7. CV of bare electrode (a) & Enzyme-APS-nanoZnO-Pt electrode (b)

3.8 Kinetic properties of enzyme bound electrode

3.8.1 Optimum pH: The response of immobilized ascorbate oxidase was determined in the pH range of 3.0-6.5 at a regular increase of 0.5. The optimum pH of immobilized enzyme was 5.5 (Fig. 8).

3.8.2 Optimum temperature: The activity of immobilized enzyme to incubation temperature was studied in the temperature range from 15°C to 45°C at a regular increase of 5°C. The optimum temperature of the present work was 40°C (Fig. 9).

3.8.3 Incubation time:

The activity of immobilized enzyme to incubation time was studied in the time range from 5 min to 35 min at a regular interval of 5 min. The activity linearly increases up to a time of 25 min and thereafter no significant increase was observed. (Fig. 10)

3.8.4 Effect of substrate concentration: Effect of trioline concentration on activity of immobilized enzyme was studied up to 500 µM (Fig. 11). Immobilized enzyme showed a hyperbolic relationship between its activity and ascorbic acid concentration up to a final concentration of 400 µM after which it was constant. The Line weaver-Burk plot for immobilized enzyme gave K_m and V_{max} values as 256.4 µM and 42.6 µM/min (Fig. 12).

3.9 Evaluation of the present method

The following parameters were studied to evaluate the performance of this method.

3.9.1 Linearity: A linear relationship was obtained ranging from 10 µM to 250 µM.

3.9.2 Minimum Detection limit: The minimum detection limit of the present method was 10 µM.

3.9.3 Analytical Recovery: In order to check the reliability of the present method, the analytical recovery of added trioline in the sample was determined (Table 1). The mean analytical recovery of added trioline (1 µM and 2 µM) in sample was 96.3% and 97.5 % respectively, which is better than recently reported method.

3.9.4 Precision: To check the reproducibility and reliability of the present method, the level of trioline content in the sample in one run (within a batch) and after storage at -20 °C for one week (between batches) were determined (Table 2). The trioline values obtained by these determinations agreed with each other and the result of within batch and between batch coefficients of variation (CVs) were < 3.82% and < 4.50%.

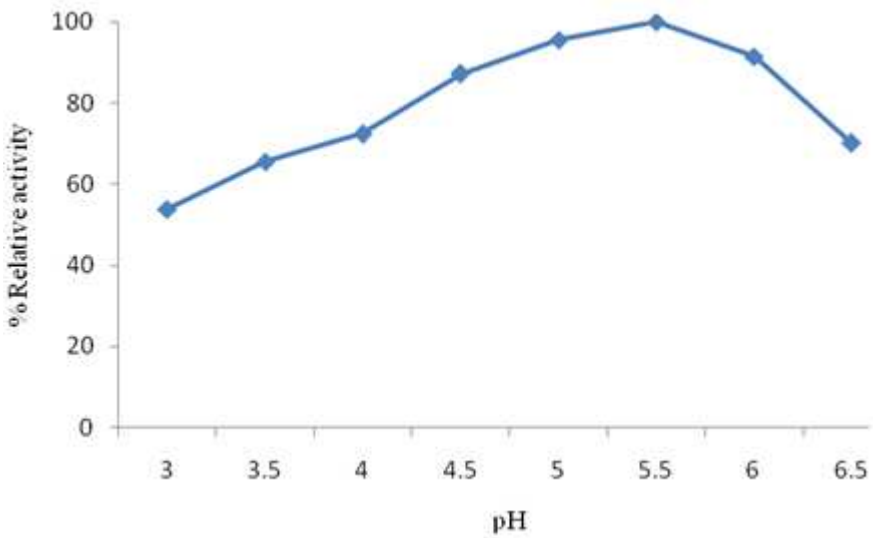

Figure 8: Effect of pH on the response of present method

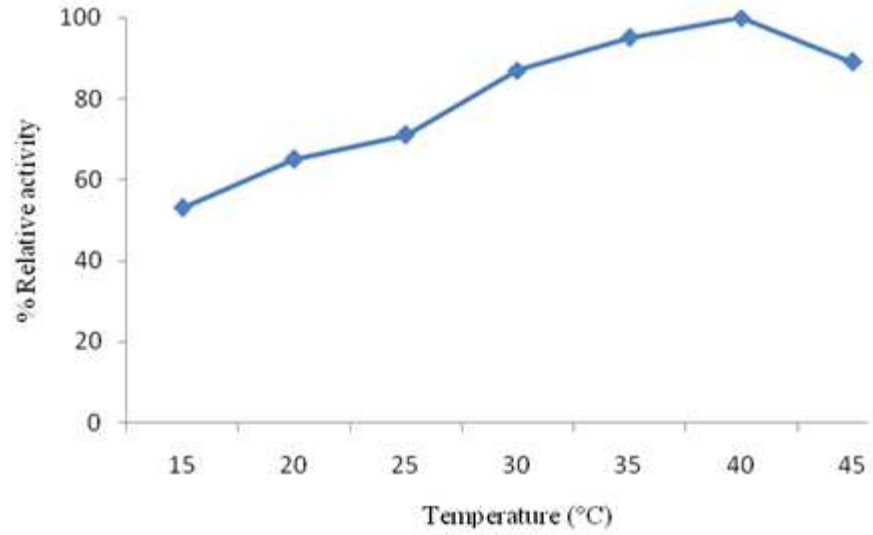

Figure 9: Effect of temperature on the response of present method

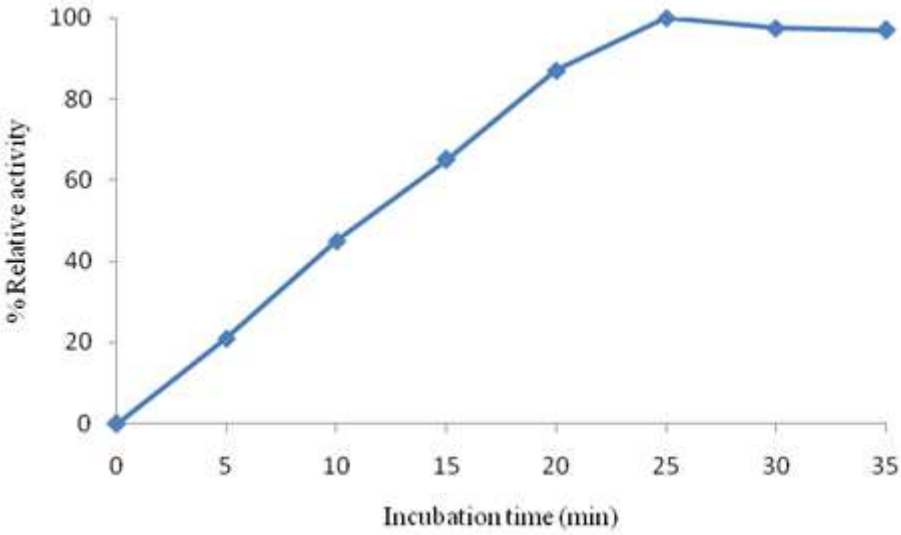

Figure 10: Effect of time of incubation on the response of present method

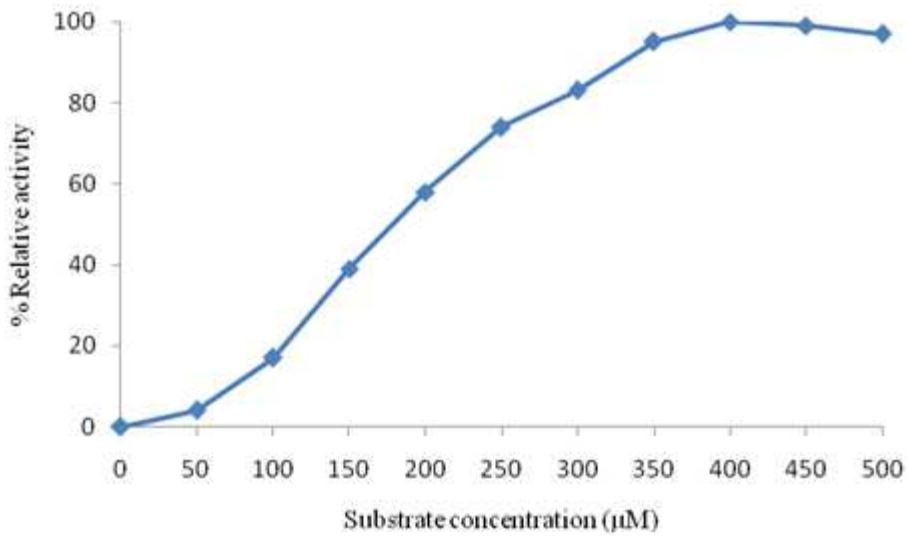

Figure 11: Effect of substrate concentration on the present method

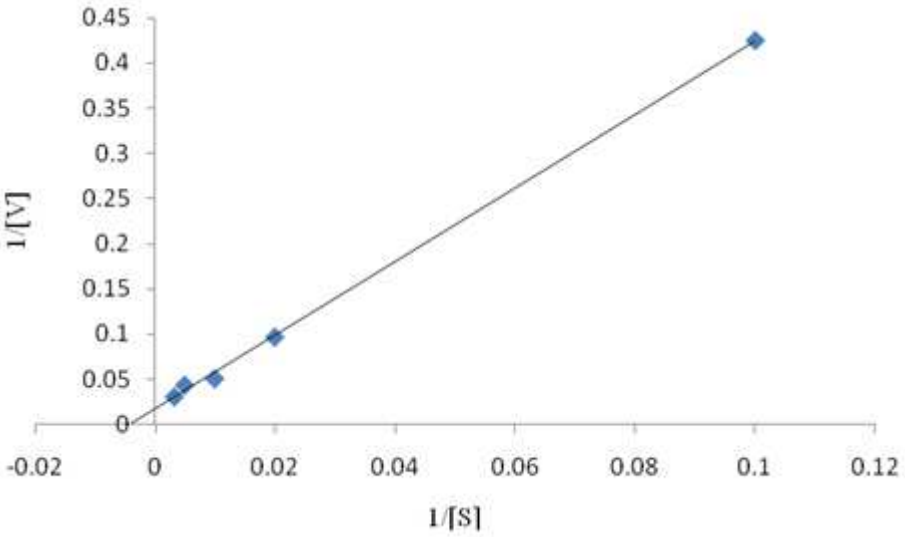

Figure 12: A Lineweaver–Burk plot between 1/[S] and 1/[v]

Table 1: Analytical recovery of added trioelin in sample

Ascorbic acid added (µM)	Ascorbic acid found (µM) Mean (n=3) ±SD	% Recovery
Nil	12.7	-
1.0	13.53±0.05	96.3
2.0	14.56±0.11	97.5

n= no. of assay

Table 2: Within and between assays coefficients of variation for determination of triolein in the sample by using enzyme bound electrode.

n	Ascorbic acid (µM) Mean ± S.D	CV (%)
Within assay (6)	12.7 ± 0.14	3.82
Between assay (6)	12.65 ±0.16	4.50

n= no. of assay

3.10 Interference study

Among the various substances investigated for possible interference to the activity of immobilized enzyme, none caused any significance interference (Table 3).

Table 3: Effect of various substances on response of immobilized enzyme

Compound added (final conc. 0.1 mM)	% Relative response
None	100
Starch	98.1
Glucose	98.8
Sucrose	97.8
Fructose	96.7
Urea	98.3

3.11 Storage stability and reusability of enzyme bound working electrode

The enzyme bound electrode lost its 50% initial activity after 50 times of regular uses over a period of 35 days when stored at 4˚C (Fig. 14a and b). The reusability and storage stability of the enzyme bound electrode was higher than earlier reported methods.

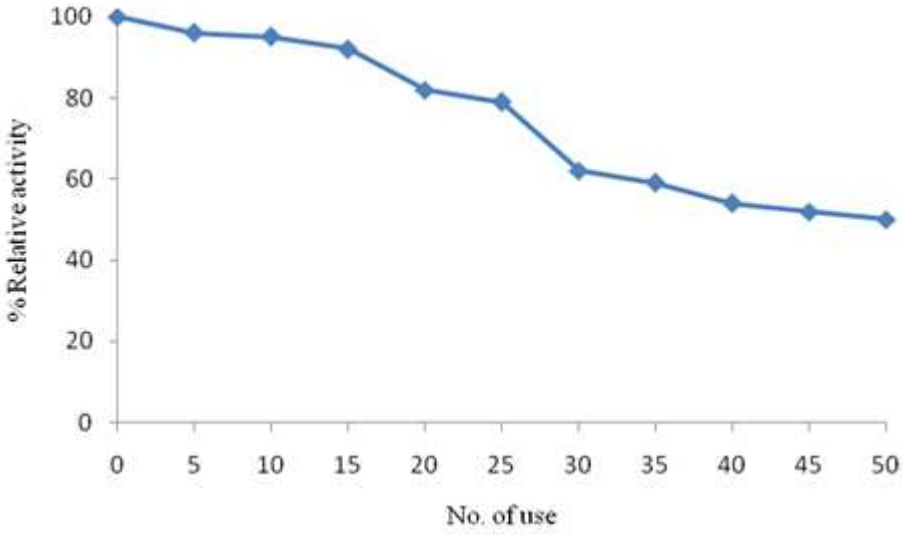

Figure 14a: Reusability of enzyme bound electrode at 4 ˚C

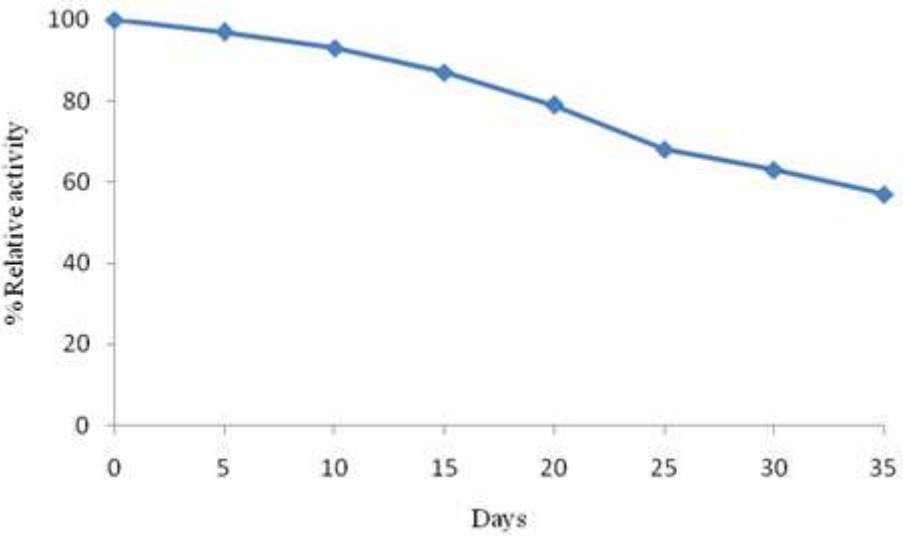

Figure 14b: Storage stability of enzyme bound electrode at 4 ˚C

CONCLUSION

By using aqueous chemical growth method zinc oxide nanorods were successfully grown on the platinum surface. UV visible spectroscopy was carried to study optical properties of synthesized nanorods and the absorbance peak was obtained at 370 nm. The crystalline structure was analysed by X-Ray diffraction and signature peaks were obtained at 31.6°, 34.2°, 36.4º, 47.4º, 56.7º, 63.2º, 66.7º, 68.2º and 69.2° which corresponded to (100), (002), (101), (102), (110), (103), (200), (112) and (201) respectively and were also found to match with JCPD card no. 089-3697. FTIR was then performed to determine chemical composition and the well-defined peaks were obtained at 520 cm^{-1},

1381 cm^{-1}, 1541 cm^{-1}, 2912 cm^{-1} and 3381 cm^{-1}. Morphological characterization by FESEM showed a visible change and growth of nanorods with the chemical synthesis at different stages. These results suggested that the method used in this study for ZnO nanorods synthesis is an easy and fast method. The immobilized enzyme showed optimum activity at pH 5.5, when incubated at 40°C for 25 min. The K_M and V_{max} for ascorbic acid was 256.4 µM and 42.6 µM/min. The linear range of the method was from 10 µM to 250 µM. The evaluation studies showed that method was reliable as mean analytical recovery of 1 µM and 2 µM were 96.3% and 97.5 % respectively and consistent as within and between CVs were 96.3% and 97.5 %, respectively. Furthermore, the method was in good correlation (0.983).

Conflict of Interest

All the authors declare no conflict of interest in the publication of this article.

Acknowledgement

The authors are thankful to Dr. Devender Jakhar; Department of Chemistry, Maharshi Dayanand University for his invaluable guidance. The authors also thank AIRF, Jawaharlal Nehru University, New Delhi for providing instrumentation facilities for FT-IR and Department of Physics, Maharshi Dayanand University, Rohtak. University of Minho, Braga, Portugal for providing FESEM facility.

REFERENCES

[1] K. G. Kanade, B. B. Kale, R. C. Aiyer, BK Das, *Mater. Res. Bull.*, **2006**, 41, 590.
[2] Z. Fu, Z. Wang, B. Yang, Y. Yang, H. Yan, L. Xia, *Mater. Lett.*, **2007**, 61, 4832.
[3] Y. Li, G. Li, Q. Yin, *Mater. Sci. Eng. B*, **2006**, 130, 264.
[4] S. Baruah, J. Dutta, Sci. *Technol. Adv. Mater.* **2009**, 10, 1.
[5] L. Miao, Y. Ieda, S. Tanemura, Y. G. Cao, M. Tanemura, Y. Hayashi, S. Toh, S. K. Kaneko, *Sci. Tech. of Adv. Mater.*, **2007**, 8, 443.
[6] H. Fissan, W. Höllander, W. Schütz, K. Okuyama, *J. Aerosol. Sci.*, **1991**, 22, 7.
[7] K. Okuyama, I. W. Lenggoro, N. Tagami, S. Tamaki, N. Tohge, *Mater. Sci.* **1997**, 32, 1229.
[8] D. C. Reynolds, D. C. Look, B. Jogai, J. E. Hoelscher, R. E. Sherriff, M. T. Harris, *Appl. Phys.* **2000**, 88, 2152.
[9] D. E. Arthur, A. Jonathan, P. O. Ameh, C. Anya, *Int. J. Ind. Chem.*, **2003**, 4, 1.
[10] P. Pramanik, S. Bhattacharya, *Mater. Res. Bull.*, **1990**, 25, 15.
[11] K. Keis, L. Vayssieres, S. E. Lindquist, A. Hagfeldt, *Nano. Mater.*, **1999**, 12, 487.
[12] J. Kim, K. Yong, *Phys. Chem.*, **2011**, 115, 7218.
[13] Z. L. Wang, Adv. *Fund. Mater.*, **2008**, 18, 3553.
[14] M. Ahmad, C. Pan, Z. Luo, J. Zhu, *J. Phys. Chem. C*, **2010**, 114, 9308.
[15] N. H. Alvi, M. Syed, U. Ali, S. Hussain, O. Nur, M. Willander, *Scripta. Materialia.*, **2011**; 64, 697.